# ACCURATE RECONSTRUCTION OF RAIN FIELD MAPS FROM COMMERCIAL MICROWAVE NETWORKS USING SPARSE FIELD MODELING

*Yoav Liberman, Hagit Messer*

Tel Aviv University
School Of Electrical-Engineering
Tel Aviv, Israel

**ABSTRACT**

Recently, it has been demonstrated that Commercial Microwave Networks (CMN) can be considered as an opportunistic sensor networks for rainfall monitoring, and in particular, for rain fields reconstruction. While different rainfall mapping techniques have been proposed, their absolute performance has never been evaluated. This paper presents a novel algorithm, which generates an accurate reconstruction of rain field maps, given measurements from commercial microwave links (ML). The accuracy is achieved by using the sparse properties of the rain field, which enables an optimal and unique recovery of the rain rates along the ML, under certain regularity conditions. We demonstrate that the performance of the proposed algorithm is close to the actual measurements of the rain intensity in a given location, and that it outperforms the reconstruction done by the Radar, almost uniformly. The proposed approach is not restricted to the specific application of rainfall mapping. It can also be used for reconstructing images, especially sparse images, which are sampled by projections on arbitrary lines.

***Index Terms—*** Rain field mapping, Image reconstruction, Microwave links, Sparsity.

## 1. INTRODUCTION

The major atmospheric phenomenon affecting the propagation of a wireless microwave signal's strength, also known as RSL (received signal level), is precipitation (mainly rain). The well-known empirical attenuation-rain rate relation is given by [1]:

$$A = \alpha R^{\beta} L \tag{1}$$

where $A$ (expressed in $dB$) is the measured RSL and $R$ (expressed in $mm/h$) is the path average rain rate along the microwave link. $L$ (expressed in $km$) is the link's length and $\alpha$, $\beta$ are constants, depending mainly on the link's frequency and the drop size distribution (in most cases $\beta \approx 1$), as detailed in [2].

The RSL is measured by receivers located at cellular base-stations distributed in space (see Fig. 1), with typical frequencies of 18-23 $GHz$, and lengths of 1-20 $km$. The measurements are given in a pre-set temporal resolution, with known magnitude resolution (quantization level). Since we are trying to reconstruct rain fields, we inspect only significant rain events, thus, we may assume that the measured RSL has high SNR, typical such RSL is shown in Fig. 2. The depicted signal is the actual RSL measurements of a microwave link provided by Cellcom company, after being pre-processed in order to overcome non-linearities in the RSL, as discussed in [3].

The use of CMN for rain monitoring was first suggested in 2006-[4]. Since then, the research had evolved greatly and was a subject of increasing interest (e.g., [5, 6]). The main disadvantage of all these methods, for rain fall mapping, is their ad-hoc nature, as none of them were proven to satisfy a unique and optimal solution for recovering the rain rates along the ML. Therefore, their accuracy might be questionable.

In this paper we present a novel algorithm, which can generate an accurate reconstruction of images in general, and rain field maps in particular, as long as certain regularity conditions are satisfied. One of the regularity conditions states that in order to guarantee a faithful rain field reconstruction, the distribution of the ML in space must satisfy certain spatial sampling conditions, as detailed in [7]. Moreover, an accurate reconstruction is achieved by using sparse field modeling, which can yield an optimal and unique recovery of the rain rates along the ML, or the pixels intensity along arbitrary lines in general images.

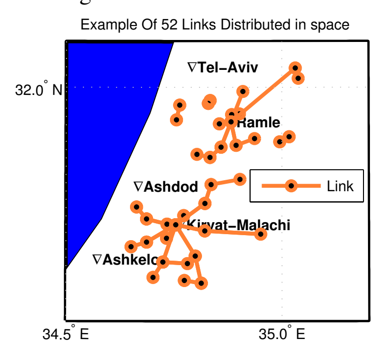


**Fig. 1**. Example of 52 links (solid lines) distributed in space, as placed by the cellular provider Pelephone, in an area of 800 $km^2$.

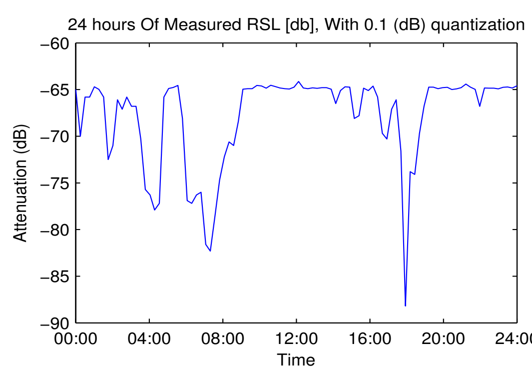


**Fig. 2**. Example of 24 hours of measured RSL ($dB$), during a rain event occurred on 07-January-2013, for a single 14 km link, operating in frequency of 21 $GHz$.

This paper is organized as follows: in Section 2 we demonstrate

978-1-4799-2893-4/14/$31.00 

our new algorithm for optimal and unique recovery of the rain rates along the ML, using sparse representation of the rain field. In Section 3 we illustrate some interesting results, along with the proposed algorithm performance. We conclude with a discussion and an alternative use of the proposed technique in Section 4.

## 2. OPTIMAL AND UNIQUE RAIN RATE RECOVERY

For any given set of RSL measurements from ML, the goal is to construct the most accurate approximation of the rain rates along the microwave links, and then to reconstruct the rain field in the links vicinity. Suppose we have a set of observed rainfall-induced RSL attenuations from $M$ microwave links in a given geometry (denoted as $A_j$, for $j = 1, ....M$). We offer to modify (1), so that each link's RSL may be written as:

$$A_j = \alpha_j R_j^{\beta_j} L_j \approx \int_{L_j} \alpha_j r^{\beta_j}(x) dx \tag{2}$$

Where $r(x)$ (expressed in $mm/h$) is the true instantaneous rain rate in a point $x$ (along the link), $L_j$ (expressed in $km$) is the $j_{th}$ link length, and $\alpha_j,\ \beta_j$ are the known $j_{th}$ link constant parameters (as described in [2]). Now, by dividing each link into $n_j$ (small enough) equal segments, we may approximate the integral in (2) and derive the following non-linear relation between each link's RSL and the actual rain rate along it (i.e., along an arbitrary line in space):

$$A_j \approx \alpha_j \sum_{i=1}^{n_j} r_{ij}^{\beta_j} l_{ij} \tag{3}$$

Where $l_{ij}$ is defined as the length of the $i_{th}$ segment for the $j_{th}$ link, and $r_{ij}$ is the unknown rain rate in each $l_{ij}$ segment. Thus, by rearranging (3), we may derive the following relation:

$$q_j(\vec{r}_j) \triangleq A_j - \alpha_j \sum_{i=1}^{n_j} r_{ij}^{\beta_j} l_{ij} \approx 0 \tag{4}$$

Where in (4) we define: $L_j = \sum_{i=1}^{n_j} l_{ij}$ and $n_j = \lfloor L_j / l_{ij} \rfloor$, which are regarded as the link's length and the total number of segments (for each $j_{th}$ link), respectively. $\vec{r}_j$ is defined as the overall $n_j$ rain rates, corresponding to each $i_{th}$ segment, along each $j_{th}$ link. Thus, in order to achieve both good spatial resolution along the links, and to yield an accurate approximation for the integral in (2), $l_{ij}$ was chosen to be $\sim 150\ (meters)$, so that: $l_{ij} << L_j$. Since each link's length varies between 1-20 $km$, each $n_j$ varies between 6 to 133 segments. It is emphasized in the sequel that $q_j(\vec{r}_j)$ (as in (4)) is a function of the unknown rain rates along each $j_{th}$ link, where the links are distributed in an arbitrary manner in space (e.g. in Fig. 1).

Hence, by defining $\vec{q} = [q_1, q_2 \dots q_M]^T$, we offer to apply the Newton-Raphson iterative algorithm (as proposed by [8]) on (4) and derive the following linear relation:

$$\frac{d\vec{q}}{d\vec{r}} |_{\vec{r}=\vec{r}_t} (\vec{r}_{t+1} - \vec{r}_t) = \mathbf{J}(\vec{r}_t)(\vec{r}_{t+1} - \vec{r}_t) = -\vec{q}(\vec{r}_t) \tag{5}$$

where for each iteration number $t$: $\vec{r}_t = [r_{t;1}, r_{t;2} \dots r_{t;N}]^T$ is known and it is defined as all the $N$ rain rates along all $M$ links in space, which are used for calculating the Jacobian matrix - $\mathbf{J}(\vec{r}_t)$ and the unknown rain rates - $\vec{r}_{t+1}$. We point out that an initialization is required as well (i.e., $\vec{r}_0$). A possible $\vec{r}_0$ can be regarded as the mean rain rate (as defined in (1)) for each one of the elements in $\vec{r}_0$, that is, for each $i_{th}$ segment along each $j_{th}$ link: $r_{ij;t=0} = (A_j)^{\frac{1}{\beta_j}} / \alpha_j$.

Thus, by rearranging (5), we may formulate the following linear system of equations:

$$\mathbf{J}(\vec{r}_t)\vec{r}_{t+1} = \mathbf{J}(\vec{r}_t)\vec{r}_t - \vec{q}(\vec{r}_t) \tag{6}$$

where (6) is solved iteratively until: $\vec{r}_{t+1} \to \vec{r}_t$. In other words, a solution for the unknown rain rates along the links is obtained when: $\|\vec{r}_{t+1} - \vec{r}_t\|^2 \leq \epsilon$ (for some pre defined small enough $\epsilon$, e.g. $\epsilon = e^{-6}$). In the sequel, by defining: $D \triangleq \mathbf{J}(\vec{r}_t)$ , $\vec{x} \triangleq \vec{r}_{t+1}$ and $b \triangleq \mathbf{J}(\vec{r}_t)\vec{r}_t - \vec{q}(\vec{r}_t)$, we may substitute the latter into (6) in order to derive the following, compact, linear system of equations:

$$\mathbf{D}\vec{x} = \vec{b} \tag{7}$$

Since each link is divided into $n_j$ segments, the system of equations derived in (7) is an underdetermined set of linear equations. Thus, there are more unknown variables to calculate (denoted as $N$) than given equations (denoted as $M$), which indicate the number of distributed links in space. This fact implies that an infinite number of possible solutions is obtained, so conventional methods such as: LS, WLS would not work [9]. Hence, a different approach is vital.

We offer to solve (7) in a new and sophisticated manner. We propose to use the fact that the rain field is generally represented in a sparse manner, as vastly cited in the literature (e.g., [10]). Namely, to some extent of the rain field, it is reasonable to assume that the rain field is mostly depicted in a sparse manner. Thus, we can assume that the solution for $\vec{r}_{t+1}$ (denoted as $\vec{x}$ in (7)) would be a sparse solution. Therefore, the best choice would be to solve the optimization "$\mathbf{L_0}$ **problem**" [11]:

$$L_0 : min\ \|\vec{x}\|_0, \text{ subject to: } \mathbf{D}\vec{x} = \vec{b} \tag{8}$$

where $\|\vec{x}\|_0 \triangleq \sum_{i=1}^{n} |x_i|^0$ ($0^0 \triangleq 1$).

As previously mentioned, because the goal is to yield an optimal and unique solution for the rain rates along the ML, we state the following theorem regarding the solution of the $L_0$ problem:

**Theorem 2.1** *If a candidate solution for $\mathbf{D}\vec{x} = \vec{b}$ has fewer than $\frac{1}{\mu(\mathbf{D})}$ nonzero elements, then it is necessarily the sparsest one possible, and any other solution must be denser.*

Where in **Theorem 2.1**, $\mu(\mathbf{D})$ is defined as the mutual coherence of the matrix $\mathbf{D}$, which is given by:

$$\mu(\mathbf{D}) = \max_{i,j} \frac{|\mathbf{D}(:,j)^T||\mathbf{D}(:,i)|}{\|\mathbf{D}(:,i)\|_2 \|\mathbf{D}(:,j)\|_2} \tag{9}$$

Where $\mathbf{D}(:,i)$ is the $i_{th}$ column of matrix $\mathbf{D}$, and $()^T$ indicates the Transpose operator. The proof of **Theorem 2.1** can be found in [11].

Since it is almost impossible to solve (8), we suggest solving the optimization "$\mathbf{L_1}$ **problem**", which also encourages a sparse solution (as detailed in [11]), therefore it conforms to our problem for finding a sparse representation of the rain rates along the ML (i.e., for finding a sparse solution for $\vec{r}_{t+1}$):

$$L_1 : min\ \|\vec{x}\|_1, \text{ subject to: } \mathbf{D}\vec{x} = \vec{b} \tag{10}$$

where $\|\vec{x}\|_1 \triangleq \sum_{i=1}^{n} |x_i|$. Solving (10) is much easier, and many methods had been proposed to solve this kind of problem (e.g., L1magic , L1Ls etc. [12]). In order to ensure a unique, optimal recovery of the rain rates along the ML, we state the following theorem regarding the $\mathbf{L_1}$ **problem**:

**Theorem 2.2** *If a candidate solution for $\mathbf{D}\vec{x} = \vec{b}$ has fewer than $\frac{1}{2}(1 + \frac{1}{\mu})$ non-zeros elements, then it is necessarily the unique optimal solution both for the $L_0$ and the $L_1$ problems.*

The proof of **Theorem 2.2** can also be found in [11].

If **Theorem 2.2** condition is satisfied (for some solution), then that solution is the optimal and unique solution of the problem at hand. In case a solution satisfying the sparse condition could not be reached, we may either use a transformation (e.g. wavelets transform) [11], or (if the data is available) we may increase the radius of the inspected area and use additional ML, so a sparser solution is more reasonable.

The next step is to construct a 2D rain field map from the estimated set - $\vec{r}_{t+1}$. That could be achieved by using either parametric, or non-parametric interpolation methods. Regarding the parametric interpolation, we use a deterministic 2D Gaussian function for the rain field modeling (with unknown parameters, e.g., unknown Variance). Afterwards, we choose the model parameters which minimizes the sum of square difference between the derived model and the actual measurements in space, which were obtained by solving (10). The 2D reconstruction might be considered as perfect (or near perfect), under certain sampling conditions, as further detailed in [3].

## 3. RESULTS

In this section we demonstrate the use of the proposed method for creating accurate 2D rain field maps, using real RSL measurements, which are available in different time and magnitude resolutions. The reconstruction is compared with Radar maps, provided by the Israeli Meteorological Service (IMS), which are available in a temporal resolution of 5 minutes. Rain gauges, which are considered as "ground truth" rain measurement instruments, are also provided by the IMS and are available in a temporal resolution of 10 minutes. Each rain gauge provides measurements of the amount of rain (in $mm$) in a certain amount of time, per square meter in space. In this paper we **analyze two rain events** which occurred in Israel in the last 3 years around Ramle ($34.88^o E, 31.93^o N$) region, with the following available data from the microwave links:

1. 18/January/2010: 26 operating ML, for a 24 hours of rain event. The RSL measurements are available in a time resolution of 1 minute, with magnitude resolution of 1 $[dB]$. The RSL measurements are provided by Pelephone.
2. 7-10/January/2013: 12 operating ML, for a 96 hours of rain event. The RSL measurements are available as Min/Max samples every 15 minutes time interval, with magnitude resolution of 0.1 $[dB]$. The measurements undergo a preprocessing stage, as detailed in [3]. The RSL measurements are provided by Cellcom.

For each event we show an example of instantaneous snapshot (as illustrated in Fig. 3) of the rain field reconstruction (in $mm/h$), on an area of about 400 $km^2$, derived by: the proposed algorithm (using ML), the rain gauges, and the Radar. In Fig. 4 we demonstrate the accumulated amount of rain (expressed in $mm$), for the two events, given: the Radar (solid line), rain gauges (dashed line) and the proposed algorithm using ML (dashed-dot line). It is obvious that the performance of the proposed algorithm follows the actual rain measurements closely in the inspected coordinate, while the Radar provides overestimation of the rainfall in the same spot.

Table. 1 summarizes the performance analysis of the Radar and the proposed algorithm once compared to the rain gauge in Ramle coordinate. The inspected measures are: (1) Correlation; (2) Root Mean Square Error (RMSE); (3) Relative Error (RE). Since each method is available in a different time resolution, we regard (for the performance evaluation) **only the instantaneous rain rates reconstructions**, derived at the common times of all methods, that is, every 30 minutes (i.e. at: 00:00,00:30...23:30).

**Table 1**. Performance Analysis Table

| event (1) | | | |
|---|---|---|---|
| | Correlation | RMSE $(mm/h)$ | RE |
| Proposed Algorithm | 0.87 | 2.07 | 2.85% |
| Radar | 0.70 | 14.32 | 20.3% |
| event (2) | | | |
| | Correlation | RMSE $(mm/h)$ | RE |
| Proposed Algorithm | 0.77 | 5.95 | 7.62% |
| Radar | 0.67 | 12.18 | 16.65% |

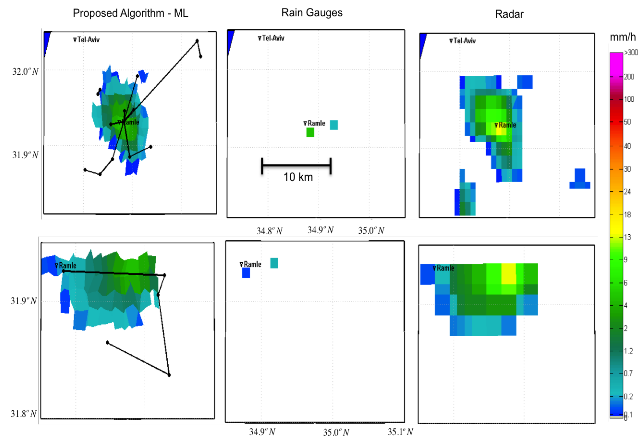


**Fig. 3**. Snapshots of the reconstructed rain fields - upper figures: event (1), 18/January/2010, at 09:30 am; lower figures: event (2), 09/January/2013, at 16:00 pm. The operating ML are depicted by black lines on the maps (left figures). Measurements from 2 rain gauges are available (middle figures), and Radar maps of the same snapshots are also provided (right figures).

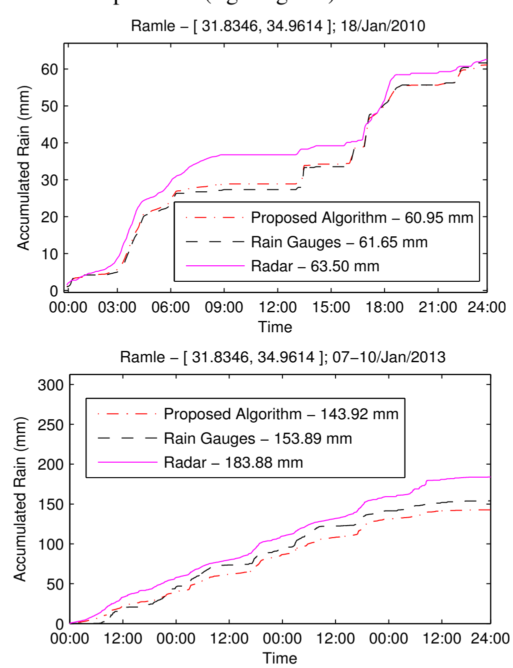


**Fig. 4**. The accumulated rain (in $mm$) in Ramle, for the two events, derived by: The proposed algorithm, the rain gauges and the Radar. Upper figure: event (1) ; Lower figure: event (2).

## 4. DISCUSSION

A new method for rain field reconstruction from CMN is presented. The method can yield a unique and optimal recovery of the rain rates along the ML, given RSL measurements from CMN. The method uses a nonlinear model linking between the RSL measurements and the rain rates along the ML. Thus, by using a linearization procedure and by utilizing the fact that the rain field is generally represented in a sparse manner, we could recover an optimal and unique solution for the rain rates along the ML, by solving the $L_1$ optimization problem, as long as the following **conditions** are satisfied:

1. The distribution of the links in space satisfy the spatial sampling conditions proposed by [7]. Hence, ensuring a faithful rain field reconstruction from the microwave links.
2. The sparse condition specified in **Theorem 2.2** is satisfied. Thus, allowing a unique and optimal recovery of the rain rates along the microwave links.
3. The RSL measurements can be regarded as high SNR data for rainfall mapping (e.g. in Fig. 2).

This paper also demonstrates some real data results and performance analyses for rainfall mapping. The comparison was done between the proposed method and the Radar, for two main rain events in a given location (Ramle). The results were conclusive: the proposed method managed to outperform the Radar reconstruction in all inspected measures, once comparing to actual rain intensities. In both inspected events, the proposed algorithm showed an improvement in: the correlation measure - about 10-17%; the RMSE - about 7-13 $(mm/h)$; and the RE - about 9-16%.

For event (2), though we achieved much better results than that of the radar, condition (1) was not satisfied due to the rather sparse network deployed in space, as shown in Fig. 3. Thus, a faithful reconstruction from the ML could not be guaranteed, where in event (1) it could, which may explain the finer performance achieved for event (1) when using the proposed algorithm. Moreover, Condition (2) was satisfied in about 90% of the inspected time periods, for both events. Thus, not only proving the rightness in using the sparsity of the rain field, but also explaining the errors occurred in the performance analysis, i.e., the remaining 10%, which did not satisfy condition (2). In both events condition (3) was satisfied.

The method proposed here can be further extended for reconstruction of general images (especially sparse images), when sampled by projections on arbitrary lines, namely, some relation between the image's pixels, along arbitrary lines is known (e.g. in (3)). We point out that an accurate reconstruction of a given image is possible if conditions (1,3), from above, are satisfied. A possible application for such scheme can be very beneficial (for example) in image compression.

The example in Fig. 5 demonstrates how the proposed method manages to achieve a near perfect reconstruction of a 256X256 image. In the example presented, a linear relation between the pixels intensity (along 50 arbitrary lines) is given by: $P_k = \sum_{i,j} p_{ij;k}$. Where each $P_k$ $(k = 1, 2 \dots 50)$ indicates a linear summation of all the pixels (denoted as $p_{ij;k}$) along each $k_{th}$ arbitrary line.

Fig. 5 depicts the reconstruction achieved from arbitrary lines (for a rather sparse image), once using our proposed method. In the image, the black lines indicate the arbitrary lines, in which the sum of all pixels, along each line, is known. The reconstruction managed to achieve a correlation (with respect to the original image) higher than $0.99$, and RMSE lower than $e^{-6}$.

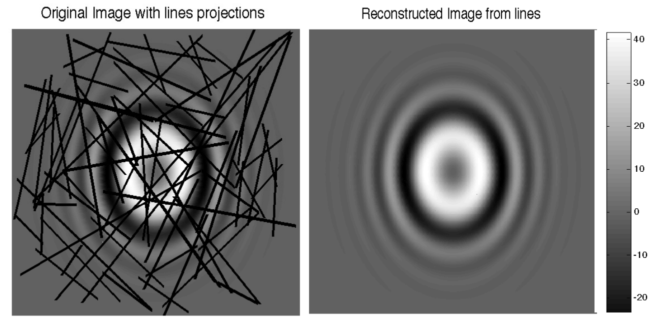


(a) Original image (b) Reconstructed image

**Fig. 5**. Example of an image reconstruction from a known linear function along projections on arbitrary lines. Figure (a): the original image with its corresponding lines. Figure (b): The reconstruction achieved by using the Proposed Algorithm

## 5. REFERENCES

[1] R. Olsen, "The $\alpha r^\beta$ relation in the calculation of rain attenuation," *IEEE Transaction, Antennas Propagation*, vol. 26, no. 2, pp. 318–329, 1978.

[2] T. Örs, Y. Chotikapong, and Z. Sun, "Bisante deliverable 2.2," *GEO Satellite Network Characteristics*, March 1999.

[3] Y. Liberman, "Optimal recovery of rain field maps using wireless sensors network," M.Sc. Thesis, Tel Aviv University, October 2013.

[4] H. Messer, A. Zinevich, and P. Alpert, "Environmental monitoring by wireless communication networks," *Science*, vol. 312, no. 5774, pp. 713–713, 2006.

[5] O. Goldshtein, H. Messer, and A. Zinevich, "Rain rate estimation using measurements from commercial telecommunications links," *IEEE T. Signal Processing*, vol. 57, no. 4, pp. 1616– 1625, 2009.

[6] A. Overeem, H. Leijnse, and L.R. Uijlenhoet, "Country wide rainfall maps from cmn," *PNAS*, March 2013.

[7] O. Sendik and H. Messer, "On the reconstructability of images sampled by random line projections," in *Electrical & Electronics Engineers in Israel (IEEEI), 2012 IEEE 27th Convention of*. IEEE, 2012, pp. 1–5.

[8] A. Ben-Israel, "A newton-raphson method for the solution of systems of equations," *Journal of Mathematical analysis and applications*, vol. 15, no. 2, pp. 243–252, 1966.

[9] H. Toutenburg et al., *Linear models and generalizations: least squares and alternatives*, Springer, 2008.

[10] E. Morin, D.C. Goodrich, R.A. Maddox, X. Gao, H.V. Gupta, and S. Sorooshian, "Spatial patterns in thunderstorm rainfall events and their coupling with watershed hydrological response," *Advances in Water Resources*, vol. 29, no. 6, pp. 843–860, 2006.

[11] S.S. Chen, D.L. Donoho, and M.A. Saunders, "Atomic decomposition by basis pursuit," *SIAM journal on scientific computing*, vol. 20, no. 1, pp. 33–61, 1998.

[12] M. Elad, *Sparse and redundant representations: from theory to applications in signal and image processing*, Springer, 2010.